A Comparison of Thiessen Polygon, Kriging, and Spline Models of Potential UV Exposure

Zaria Tatalovich, John P. Wilson, and Myles Cockburn

ABSTRACT: The performance accuracy of Thiessen-polygon and kriging interpolation methods available in the standard GIS packages was evaluated based on magnitude of errors in predicting potential UV exposure across the continental U.S., and the results were compared with those of the ANUSPLIN routine that runs outside typical GIS through a series of C++ and FORTRAN commands. Input data consisted of global radiation measures recorded at 215 stations, latitude, longitude, and elevation from a 30 arc-second Digital Elevation Model. The objective was to identify the most accurate prediction method for facilitating measurement of potential UV exposure at local (e.g. 1km^2 grid cell) and county levels. The ANUSPLIN method produced the smallest prediction errors in estimating values of potential UV exposure at 1 km^2 resolution; these measurements were aggregated to the county level. We examined how much variation was lost through aggregation, as well as the potential bias associated with the possibility that some counties have predominantly north or south facing slopes. The impact of using inferior procedures on the estimates and geographic patterns of potential UV exposure was also examined. ANUSPLIN generated results that are reproducible and for which uncertainty is known. These measurements will be used in subsequent analysis of the role of UV exposure in melanoma etiology.

Introduction

The reasons for measuring potential ultraviolet (UV) exposure correspond to concerns about health and environment. Prolonged exposure to UV radiation has specific effects on human health, crops, terrestrial ecosystems, and aquatic ecosystems (Tevini 1993; Caldwell and Flint 1994). In humans, UV exposure is critical for understanding melanoma etiology (Elwood 1989; Armstrong and Kricker 1993; Elwood and Koh 1994; Elwood and Jopson 1997; De Fabo et al. 2004) and other common adverse effects, such as conjunctivitis and sunburn (De Gruijl 1997). Measurement of UV exposure, however, has proved challenging. Often, the assessment of the health effects resulting from UV exposure fails to provide useful results due to incomplete exposure measurements.

Zaria Tatalovich, Department of Geography, University of Southern California, Los Angeles, CA 90089-0255. Tel: 213.821.1313; Fax: 213.740.0056; E-mail: <tatalovi@usc.edu>. **John P. Wilson**, Department of Geography, University of Southern California, Los Angeles, CA 90089-0255. Tel: 213.740-1908; Fax: 213.740.9687; E-mail: <jpwilson@usc.edu>. **Myles Cockburn**, Department of Preventive Medicine, University of Southern California, Los Angeles, CA 90089-9175; E-mail: <myles@ccnt.hsc.usc.edu>.

Measurement of UV exposure at specific body sites has been accomplished using personal passive UV dosimeters (Diffey 1989) which quantify the distribution and the fraction of the ambient UV radiant exposure on a horizontal plane. However, this method, while useful for measuring current individual exposures cannot be used to measure the effects of historical UV exposure (Holman and Armstrong 1984; Autier and Dore 1998). The impact of historical exposure is typically assessed through self-report. The drawback in this subjective approach to UV exposure assessment is that results may be subject to recall bias (Cockburn et al. 2001). In an attempt to better account for historical exposure, mean annual hours of bright sunshine received at location of residence has been used as the metric of individual UV exposure (Armstrong 1988). However, this metric is not the best proxy for UV exposure because of the inconsistent relationship between incoming solar radiation and sunshine hours (see Linacre (1992) and Liou (2002) for factors that influence trends in incoming solar UV).

In recent years, the assessment of the role of historical UV exposure in melanoma etiology has increasingly relied on the interpolation of UV exposure at places of residence based on the

available solar radiation networks. Fears et al. (2002) was one of the first to objectively measure UV exposure at location of residence based on the actual UV measurements recorded by approximately 30 radiation stations across the continental U.S.A. However, a principal limitation was that the accuracy of individual UV exposure estimates was unknown. The analysis relied on interpolation of data from a small imperfect measurement network, and it may have fallen short of accurately representing spatio-temporal heterogeneity of incoming UV energy at the local level (e.g. 1km^2 grid cell). Yet, no proper attention was given to the issue of spatial variability and uncertainty in UV estimates from which measures of individual exposure were derived.

Specifically, the fact that solar radiation varies not only across different latitudes but also across different elevation gradients and various features of the receiving terrain (Wilson and Gallant 2000) has generally been overlooked in recent attempts to quantify UV exposure. Furthermore, the quality of any analysis that relies on interpolation of values at unsampled locations based on the imperfect measurement networks such as that for solar radiation is always subject to a degree of uncertainty, because the derived values are only estimates of what the real values should be at a particular location (Chiles and Delfiner 1999). Different interpolation methods can therefore generate different predictions at the same locations (see Lam (1983), Burrough (1986), Meyers (1994), Burrough and McDonnell (2000), and Cressie (2003) for reviews of different interpolation techniques).

This raises fundamental questions regarding how well potential UV exposure can be modeled, given not only the measurement network and methods available to us at this time but also the resolution of the spatial unit (e.g., place of residence, county, census tract) relevant in the analysis of individual UV exposure. Significant progress has been made in the development of solar radiation models (e.g., Solar Flux model (Dubayah and Rich 1995); SRAD model (Wilson and Gallant 2000), and Solar Analyst model (Fu and Rich 2000)) which are all suitable for fine-scale resolutions. Is it possible to develop models of UV exposure that would effectively cope with the potentially large degree of local variation at, for example, the county level? Studies are needed that will assess the performance of different source data and spatial interpolation techniques for estimating potential UV exposure and the capture of spatial variability and uncertainty in exposure estimates.

A comparison of performance accuracy of different interpolation methods available in standard geographic information systems (GIS) packages was conducted previously (Siska and Hung 2001) using a local, low-vacillating (i.e., relatively uniform) elevation data set. The results suggest that the Thiessen polygon, kriging, and Triangular Irregular Network (TIN) procedures performed almost at the same level, producing the least error in comparison to the Inverted Distance Weighting (IDW) and trend surface analysis interpolation methods. An as yet unanswered question is how would some of the procedures that were identified in this instance as more accurate perform on a non-uniform, elevation-dependent surface such as UV radiation.

In response to the aforementioned needs, the present research attempts to:

- Evaluate the performance of the Thiessen polygon and kriging interpolation procedures in a standard (GIS) package in estimating potential UV exposure across the continental U.S.; and
- Compare these results with those obtained with the ANUSPLIN (Spline) routine (Hutchinson 2003) that runs outside typical GIS through a series of C++ and FORTRAN.

The Thiessen polygon, kriging, and ANUSPLIN procedures were purposely chosen for this type of analysis because of their very different statistical properties, and also computational complexity, and their ability to incorporate additional variables, all of which may differentially affect the predictions. The impetus for stepping outside the typical GIS toolbox and using ANUSPLIN was stimulated by the success of this procedure in predicting precipitation, temperature, and other climate variables while incorporating their spatial dependence on elevation (Hutchinson 1991b; 1993; 1995; 1998; Corbett and Carter 1996; Custer et al. 1996; Stillman 1996). As a part of this effort, our research also includes:

- An examination of the impact of using this alternative methodology on the resulting patterns and estimates of potential UV exposure at the local and county levels; and
- A model for which the accuracy of measurements is known, and which can be used to facilitate objective assessment of historical and cumulative lifetime UV exposure for determining melanoma risk.

In the following section of this paper we describe (1) the measurement network and data used for input in each interpolation procedure; (2) the characteristics of the three interpolation techniques

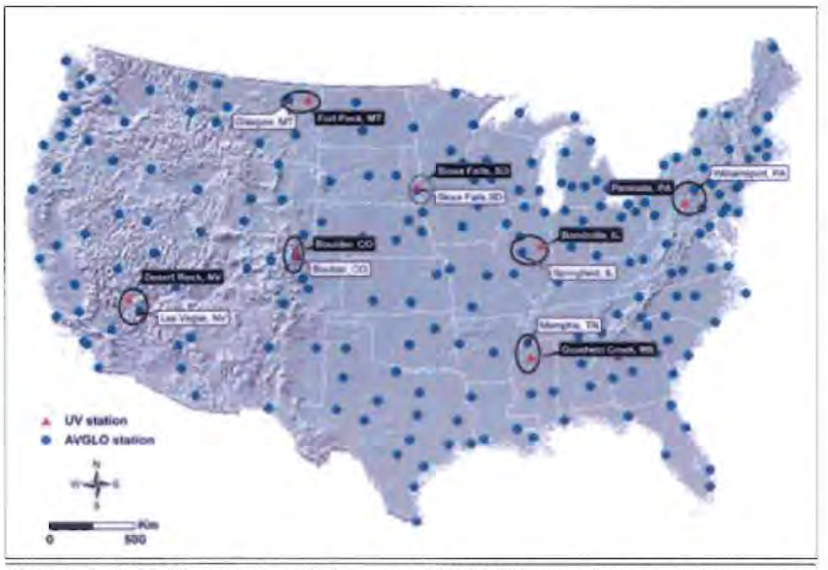

Figure 1. NSRAD global radiation and SURFRAD ultraviolet radiation station networks.

and how they were utilized to generate estimates of potential UV exposure at unsampled locations across the continental U.S.; (3) how model performance was evaluated based on the magnitude and distribution of errors; and (4) the procedures used to examine where the results diverge at the local (1km² grid cell) and county levels.

GIS technology is particularly well suited to communicate the results of this type of analysis because it enables the calculation of statistical parameters, their comparison through charts and graphs, and visualization of geographical distribution of errors via maps, as outlined in the next section of the paper. The advantages and disadvantages of the methods used are discussed in the last section, as are the effects of using alternative procedures on the estimates and geographical patterns of potential UV exposure and the uncertainties that remain once the estimates are aggregated to the county level.

Methods

Solar Radiation Data

The National Solar Radiation Database (NSRAD) produced by the National Renewable Energy Laboratory (NREL) under the Department of Energy's (DOE) Resource Assessment Program provided the input data for each interpolation procedure (described in detail in the next section). Containing statistical summaries computed from hourly data for 239 U.S radiation stations for the period 1961-1990, NSRAD is currently the largest network in the U.S. for measuring solar radiation data. The statistics include monthly, yearly, and 30-year average global solar radiation[1] measures. The decision to use 30-year averages was based on an initial analysis of temporal variability that showed no statistically significant difference in AVerage daily total GLObal solar radiation (AVGLO) measurements between the three 10-year periods embedded in the 1961-1990 data summaries for each radiation station.

AVGLO as Proxy for UV

The AVGLO measure was adopted and tested as a proxy for UV, because the spatial distribution of AVGLO data was larger and their quantity more complete than in any UV database available at this time. Monthly UVB data from the Surface Radiation Budget Network (SURFRAD) stations of the National Oceanic and Atmospheric Administration (NOAA) were used for comparison with AVGLO data at similar or nearby locations to see how well the variability in AVGLO mimicked the variability in UV.[2]

The UVB flux employed for this study is the total UVB convoluted with the erythemal action spectrum (i.e., that part of the UVB spectrum responsible for sun burns on human skin (erythema) and DNA damage). The UVB measures downloaded for this project consisted of monthly UVB averages in mW/m², covering the period 1995-2004, and recorded at seven SURFRAD stations in seven climatologically diverse states (Montana, Colorado, Illinois, Mississippi, Pennsylvania, Nevada, and South Dakota). Seven AVGLO stations were selected for the comparison based on proximity to UV stations (Figure 1). The correlation between monthly UVB and AVGLO values at nearby stations

[1] The 30-year AVerage daily total GLObal solar radiation (AVGLO) is defined as the total amount of direct and diffuse solar radiation in Wh/m² received on a horizontal surface.

[2] A detailed description of the SURFRAD database is given at: ftp://ftp.srrb.noaa.gov/pub/data/surfrad/.

was calculated to determine if global radiation measures could serve as a proxy for UV measures in the present research.

Digital Elevation Model Data

Four 30 arc-second Digital Elevation Models (DEMs) covering North America were obtained from NOAA's National Geophysical Data Center (NGDC) (see http://www.ngdc.noaa.gov/ for details). The DEMs were converted from image to grid, projected to the WGS84 geographic projection, edge-matched, and then joined in the Arc/Info 8.1 GRID module to create a single DEM. The DEM was clipped to cover only the continental U.S.; it had 9,600 columns and 3,120 rows.

Interpolation Procedures

The Thiessen polygon, kriging, and ANUSPLIN interpolation techniques were utilized to generate UV measurements at unsampled locations across the continental U.S. In each instance, the same point dataset was comprised of 215 solar radiation stations which provided the data for generating a continuous UV exposure surface with 1 km^2 grid cell resolution. The specific routine to accomplish this task differs from one interpolation method to another. Each routine also incorporated computation of prediction errors (the difference between observed and predicted values) at sampled locations. The predicted values at sampled locations were generated by systematically removing the input data for one radiation station and then calculating radiation for that station based on measurements at the other station(s). This step facilitates the analysis of the performance accuracy of each method.

Thiessen Polygons

Thiessen polygons, also referred to as Dirichlet tessellations or Voronoi diagrams, are an exact method of interpolation that assumes that the values of unsampled locations are equal to the value of the nearest sampled point. This method is commonly used in the analysis of climatic data when local observations are not available, and data from the nearest weather stations are used. Thiessen polygons define the individual "regions of influence'" around each set of points, such that any location within a particular polygon is nearer to that polygon's point than to any other point and, therefore, has the same value (Heywood et al. 1998). The Thiessen polygon interpolation method is available within most popular GIS packages, including the Environmental Systems Research Institute's (ESRI's) ArcGIS.

In this research Thiessen polygons were generated using the ArcGIS 9 toolbox command named Thiessen Polygons and point coverage representing 215 radiation stations. The input point coverage attribute information included the average global radiation (AVGLO) means for the period 1961-1990 (Wh/m^2), the station locations in decimal degrees of longitude and latitude (all derived from NSRAD), and the elevation at each station location as derived from a 30-arc second U.S. Geological Survey DEM. The resulting coverage was transferred to ArcInfo 8.1 where it was clipped to the shape of the continental U.S. and subsequently converted to a raster in the GRID module.

To derive a set of predicted global radiation values at each sampled location, a "jack-knife procedure" was used, where one data point (station) at a time was removed, and the values at each missing point were calculated based on the next nearest station. The idea was to determine how well the neighboring station estimated the missing value. The jack-knife procedure required 215 point coverages for input (each with a different missing point); the Thiessen polygon procedure was implemented with each of these coverages to predict values at the missing points. The predicted values were then recorded in the attribute table that contained the matching observed values for all data points in the original coverage. The actual, absolute, and percent differences between observed and predicted values (errors) were calculated using ArcGIS 9.

Kriging

Kriging is a geo-statistical method that uses known values and a semivariogram to predict the values at unmeasured locations. The semivariance is a measure of the degree of spatial dependence between samples. The magnitude of the semivariance between points depends on the distance between the points. With kriging, therefore, predicted values are not the same as the "source" point (like with the Thiessen polygon approach) but rather vary depending on their proximity to the source. The semivariogram model that best fits the data is developed to produce the optimum weights for interpolation (Burrough and McDonnell 2000). The derivation of this semivariogram is discussed in greater detail in Cressie (2003).

In our research, the kriging model runs were performed using the Geostatistical Analyst extension of ArcGIS 9. This extension offers several kriging models: simple, ordinary, universal, indicator, disjunctive, probability, and their multivariate equivalents in cokriging (see Johnston et al. 2001 for review of a Geostatistical Analyst). The input data consisted of the same point coverage that was used with the Thiessen polygon approach. The kriging procedures require numerous decisions in terms of choosing an appropriate kriging model, when surface trend needs to be removed (detrended), and when the neighborhood parameter needs to be adjusted.

Based on the preliminary analysis of data, we chose the Ordinary and Universal kriging models. These forms of kriging both assume normally distributed data but make different assumptions about the mean value of the variable under study. While Ordinary kriging requires a constant but unknown mean, Universal kriging assumes a spatially varying mean, and it is useful when one wants to account for the trends observed in the exploratory data analysis (Krivoruchko and Gotway 2004). The two models were run consecutively, each with different parameters, in order to arrive at the best model predictions for each model type. Detrending was performed to remove a surface trend from the data (i.e., spatial dependence of values on elevation) and Ordinary and Universal kriging was then run on the residuals to see if this intervention would significantly improve the results. The Ordinary and Universal Cokriging models (incorporating elevation as an external variable) were used for the same reason.

The ESRI *Geostatistical Analyst* extension provided an indication of which model produced minimal prediction error though cross-validation. The cross-validation procedure used all the data to estimate trend and autocorrelation models, and then removed each data location, one at a time, and predicted the associated data value. The resulting cross-validation matrix provided measures of error, absolute error, and standard error of prediction. The best model predictions were used to derive a continuous raster exposure surface with a 1 km^2 grid cell resolution.

Splines

The spline family of techniques was first described by Wahba (1980) and computationally extended by Hutchinson (1991a) for use with climate data. Thin plate smoothing splines can be viewed as a generalization of standard multivariate linear regression in which the parametric model is replaced by a suitably smooth nonparametric function. The degree of smoothness, or, inversely, the degree of complexity, of the fitted function is usually determined automatically from the data by minimizing a measure of predictive error of the fitted surface given by generalized cross validation (GCV) (Craven and Wahba 1979; Hutchinson and Gessler 1994).

Comparisons of splines and kriging are given by Hutchinson (1991b, 1993, 1995), Hutchinson and Gessler (1994), and Laslett (1994). Whereas thin plate splines are defined by minimizing the roughness of the interpolated surface with prescribed residuals from the data, kriged surfaces are defined by minimizing the variance of the error of estimation, which normally depends on the preliminary semi-variogram analysis (Hutchinson and Gessler 1994).

The ANUSPLIN package provides a facility for transparent analysis and interpolation of noisy multivariate data based on thin-plate smoothing splines (Hutchinson 2003). The package supports this process by providing comprehensive statistical analyses, data diagnostics and spatially distributed standard errors. It also supports flexible data input and surface interrogation procedures. The ANUSPLIN package is made up of eight FORTRAN and C++ programs: SPLINA, SPLINB, SELNOT, ADDNOT, DELNOT, GCV GML, LAPPNT, and LAPGRD. The approach is simple, and computer storage requirements are comparatively modest, even though the routine is computationally complex. The present study utilized two FORTRAN programs— SPLINA and LAPGRD—and both were run in conjunction with the Arc module of ArcInfo 8.1 using ASCII files for input and output.

The SPLINA program was used to calculate predictions of global solar radiation using partial thin-plate smoothing splines on the same dataset as with the kriging and Thiessen polygon methods. The SPLINA program required two input files. The first, a user-directive file, contained the following information: number of independent spline variables (2; latitude and longitude); number of independent covariates (1; elevation); lower and upper limits for longitude and latitude of the area covered by radiation stations; elevation in kilometers; order of spline (2); number of surfaces (1; radiation values); number of data points (215); and input-output parameters specified in the directive. The second ASCII file contained the annual radiation means for the period 1961-1990 (Wh/m^2), the station locations in decimal degrees of longitude and latitude (all derived from NSRAD

as described in the next section), and elevation derived from the previously described DEM.

SPLINA generated numerous diagnostics in addition to an ASCII file with surface coefficients summarizing the relationship between mean global solar radiation, latitude/longitude, and elevation. The surface diagnostics included a generalized cross validation estimate, i.e., a measure of the predictive error of the fitted surface calculated by removing each data point in turn and summing the square of the discrepancy of each omitted data point from a surface fitted to all the other data points (Hutchinson 2003). The other diagnostics were the mean square error (MSE) of the smoothed data values, the mean square residual (MSR), an estimate of mean relative error variance (VAR), and the square roots of all three variables. These measures were used to evaluate model predictions.

The LAPGRD program required three input files: a surface coefficient file output from SPLINA, a 1 km² DEM in ASCII format, and a user-directive file containing elevation and location bounds, grid cell size, special value options for cells with no data, and input–output file parameters. The program, which combines surface coefficients with DEM to estimate solar radiation values at each DEM grid node, generates an ASCII file with elevation and solar radiation estimates which are then transferred to ArcInfo 8.1 and converted to a lattice in the GRID module.

Model Evaluation

At the outset we assessed the performance accuracy of different interpolation procedures based on the magnitude and distribution of errors between observed and model-predicted values using a series of statistical measures. These measures are briefly described below.

The root mean square error (RMSE) was calculated for each model prediction using the following equation:

$$RMSE = \sqrt{SSE_i^2 / n} \qquad (1)$$

where:
SSE = the sum of the squared errors (observed minus estimated values); and
n = the number of pairs (errors).

RMSE is frequently used as an important measure of the accuracy of spatial analysis in GIS and remote sensing (Siska and Hung 2001). The mean absolute error (MAE)—the average absolute difference between observed and predicted values—and the variance of the errors (VE) were calculated using the following equations:

$$MAE = SAE_i / n \qquad (2)$$

$$VE = SSD_i / n \qquad (3)$$

where:
SAE = the sum of the absolute errors (observed minus estimated values);
n = the number of pairs (errors); and
SSD = the sum of the squared differences between the errors (observed minus estimated values) and mean error.

Large RMSE and MAE values and relatively large VE values indicate larger discrepancies between predicted and observed values. Correlation coefficients were calculated between observed and predicted values and between errors and observed values. Better model performance is indicated by higher coefficients between observed and predicted values; lower coefficients between errors and observed values are also indicative of better performance (Siska and Hung 2001). The statistical analysis of error was supplemented by a visual comparison of error statistics through maps and charts.

After completing model evaluation we examined the impact of using alternative interpolation methods on the resulting patterns of UV exposure across the continental U.S. The exposure surfaces generated by the Thiessen polygon, hriging, and ANUSPLIN routines, respectively, were compared on a cell-by-cell basis to provide an indication where the results diverged. Percentage differences between the largest and smallest values at matching 1 km² grid nodes were plotted on a map for visual comparison.

Generating County Estimates of Potential UV Exposure

As mentioned above, the objective of the analysis was to compute county estimates of potential UV exposure across the continental U.S. using the most accurate model predictions. The county-level estimates should, in turn, help facilitate the objective assessment of historical UV exposure in those instances where the county is used as a unit that describes the individual place of residence. The procedure involved calculating the mean values of all 1 km² grid nodes that belong to a particular county in the Arc/Info GRID module. The resulting exposure surface was used to generate a map of potential UV exposure by county.

Generalization of UV exposure measurements at the county level raised several concerns regarding propagation of uncertainty at the coarser resolution. One important concern was how much variation in the estimates of UV exposure was lost through aggregation. This was examined by calculating the coefficient of variation in exposure values for each county prior to aggregation, using the following equation:
where:

$$CV = \frac{S^2}{\overline{X}} \times 100 \qquad (4)$$

CV = coefficient of variation (%);
S^2 = variance; and
$\overline{X}$ = the mean value of the set.

Other issues of interest were the use of horizontal surfaces for the calculation of UV and the possibility that the presence of predominantly north- or south-facing slopes (aspects) in some counties might have introduced substantial bias in the county-level exposure estimates (e.g., Dubayah and Rich 1995; Wilson and Gallant 2000). To check if this was the case, a measure of aspect was calculated for each 1 km² cell. Because the aspect measure is circular (0°-360°), it was transformed by calculating its cosine which produces values that range from -1 (south facing) to +1 (north facing) (Copland 1998). Aspect measures were aggregated at the county level and used to categorize counties into the following five classes: >0.5 (predominantly north-facing slopes); 0.2 to 0.5 (moderately north-facing slopes); -0.2 to 0.2 (equal number of grid cells with north and south facing slopes); -0.2 to -0.5 (moderately south-facing slopes); to >-0.5 (predominantly south-facing slopes).

Generalization of the estimates to the county level invited further examination of the impact that inferior techniques might have on county exposure estimates. The Wilcoxon signed rank test was used for pair-wise comparison of the county estimates generated by the Thiessen polygon, kriging, and ANUSPLIN methods to determine if the differences in estimates were significantly different.

Results

Correlation between AVGLO and UV

The correlation between UV and global radiation values at nearby stations was evaluated to explore the option of using AVGLO measurements as proxies for UV measurements, and the results are presented in Figure 2. The first scatter plot reveals a high correlation between average annual UV and global radiation measurements at seven matching locations (r^2 = 0.90). The remaining seven scatter plots show correlation between monthly AVGLO and UV measurements for the seven station pairs. The large positive coefficients of determination obtained (r^2 > 0.97) indicate that the variability of global radiation measurements mimics the variations in UV at similar locations and could, therefore, be used as a proxy for UV in this research.

Assessment of Kriging Models

To evaluate the kriging models we used the cross-validation matrix which provided measures of average standard error, standardized mean, and absolute and standardized root mean square error. Generally, the best model is the one that has a standardized mean nearest to zero, the smallest root mean square error, an average standard error nearest to the root mean square error, and a standardized root mean square prediction error nearest to one (Johnston et al. 2001).

A comparison of the error statistics for the kriging models used is given in Table 1. The results suggest that Universal kriging and Universal cokriging performed at the same level, generating the best statistics. The Universal kriging model was selected

	Kriging		Detrended Kriging		Cokriging	
Statistics	Ordinary	Universal	Ordinary	Universal	Ordinary	Universal
Average Standard Error	159	112	118	201	163	113
Standardized Mean	-0.005	-0.009	-0.005	-0.03	-0.003	-0.006
Root Mean Square Error	104	104	108	116	112	106
Standardized Root Mean Square Error	0.63	0.89	0.88	0.56	0.67	0.9

Table 1. Error statistics for six kriging models.

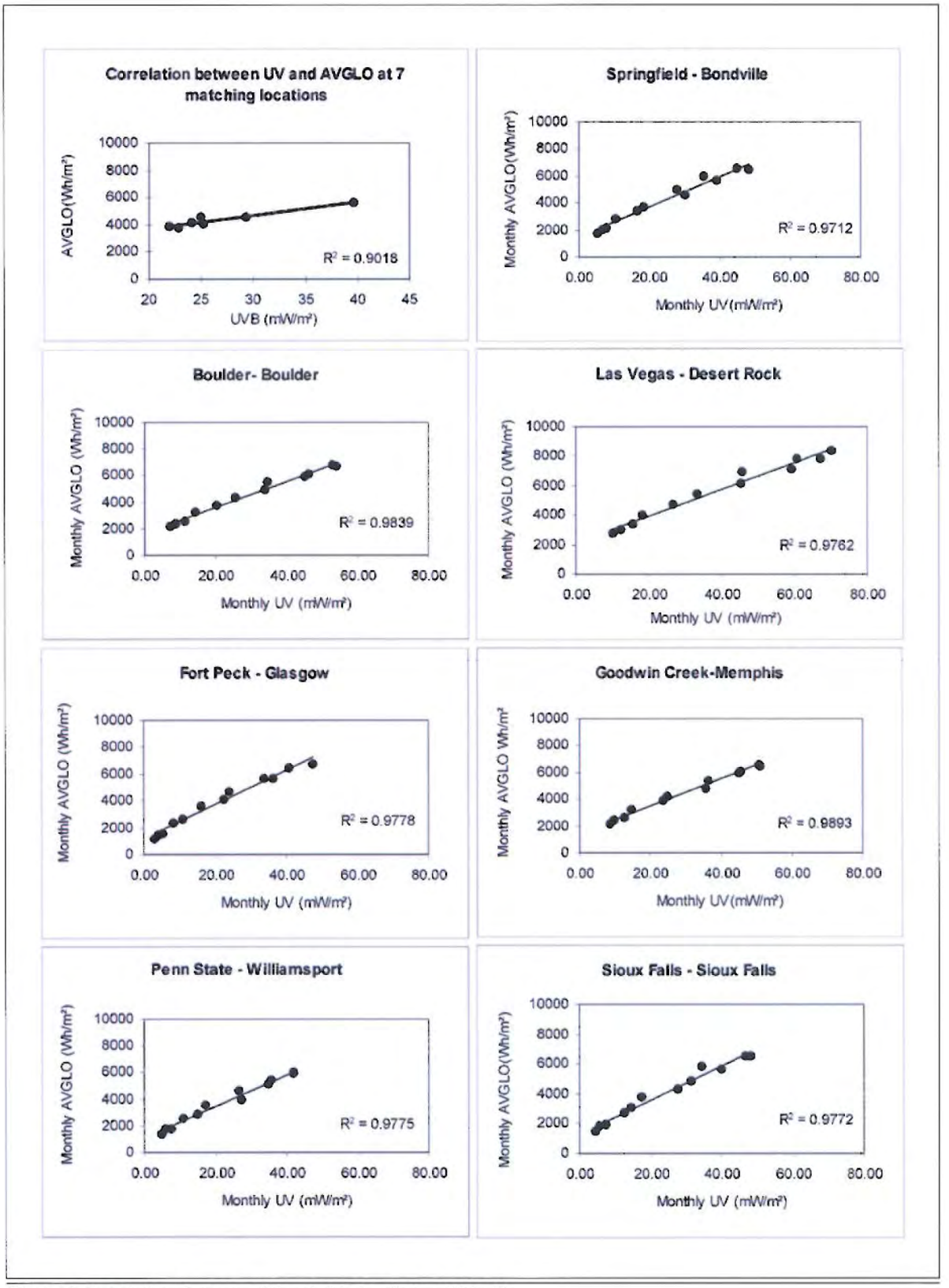

Figure 2. Correlations between UV and global radiation (AVGLO).

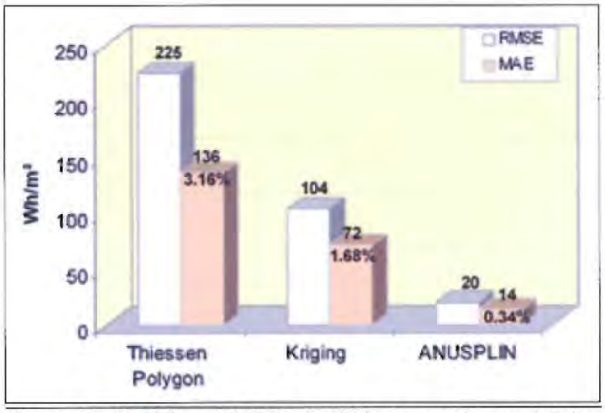

Figure 3. RMSE and MAEs for Thiessen polygon, kriging, and ANUSPLIN predictions.

for comparisons with the Thiessen polygon and ANUSPLIN models because the model generated a slightly lower root mean square error.

Accuracy of Thiessen Polygon, Kriging, and ANUSPLIN Prediction Models

The analysis of the RMSE statistics for all three models suggests that ANUSPLIN yielded the smallest errors while the Thiessen polygon method generated the highest RMSE. The ANUSPLIN interpolation was 11.25 times more accurate than the Thiessen polygon and 2.2 times more accurate than the Universal kriging method using this metric as a guide (Figure 3).

Similarly, the mean absolute error values indicate that ANUSPLIN performed better than the Thiessen-polygon and Kriging for this application. The ANUSPLIN error was 14.2 Wh/m² (0.34%), whereas the Universal kriging method generated a MAE of 72.5 Wh/m² (1.68%), and the Thiessen polygon interpolation method yielded a MAE of 136 Wh/m² (3.16%). The ANUSPLIN model also generated the smallest VE, whereas the Thiessen polygon predictions yielded the highest. Both measures confirm that ANUSPLIN produced the smallest uncertainties in predicting values at known locations (Table 2). Not surprisingly, the ANUSPLIN routine also produced the highest correlation coefficient between observed and predicted values and the lowest correlation coefficient between errors and observed values.

A visual comparison of the geographic distribution of errors for the three models helped identify the location of the largest prediction errors (Figure 4). For the Thiessen polygon interpolation, the largest errors occurred for those radiation stations that are located in areas with sharp differences in elevation. The absolute errors ranged between 0.5 percent and 16 percent. A similar pattern was generated with the Universal kriging model, although the predictions were generally better with errors ranging from 0 to 13 percent. In contrast, the errors produced by the ANUSPLIN model were relatively uniformly distributed across the region and never exceeded 1.7 percent.

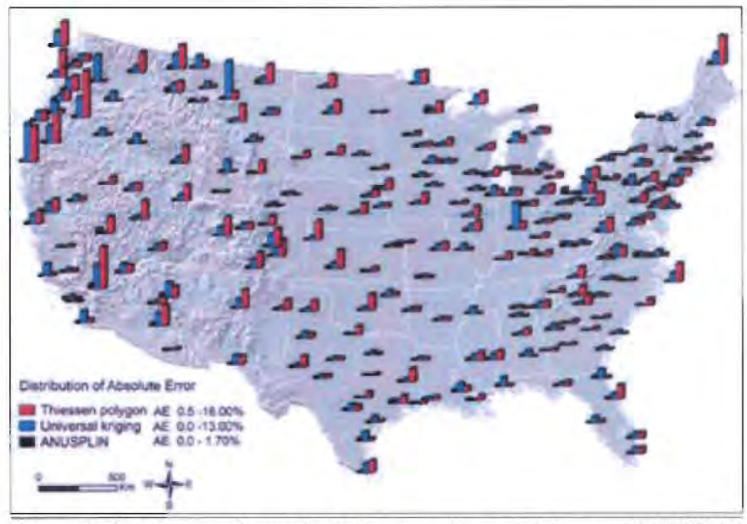

Figure 4. Distribution of error for Thiessen polygon, kriging, and ANUSPLIN predictions.

Models	RMSE	MAE	VE	Correlation OBS/PRED	Correlation OBS/ERR
Thiessen-Polygon	225	136 (3.16%)	50906	0.90	0.40
Universal Kriging	104	72 (1.68%)	10885	0.98	0.31
ANUSPLIN	20	14 (0.34%)	384	0.99	0.15

Table 2. Error statistics for Thiessen polygon, kriging, and ANUSPLIN predictions.

The scatter diagrams presented in Figures 5a, 5b, and 5c supplement the aforementioned results by showing the differences in absolute errors and elevation for each of the three model predictions. These diagrams reveal that the errors generated by ANUSPLIN are relatively uniformly distributed across dif-

ferent elevation gradients, in contrast to errors produced by the Thiessen polygon and kriging procedures, both of which have non-uniform dispersal across the elevation matrix.

Model Comparison

The impact of the Thiessen polygon, kriging, and ANUSPLIN procedures on the geographic patterns of potential UV exposure is demonstrated in Figure 6 (a, b, and c, respectively). The three models have similar regional patterns of potential UV exposure; however, there are some subtle differences (at least they appear subtle at the current scale) that warranted further examination.

A cell-by-cell analysis of the differences between the three exposure surfaces was performed to identify where the largest discrepancies in the UV estimates occurred. As Figure 7 reveals, UV values diverge more substantially in the western U.S., in those areas where there are sharp differences in elevation. These findings are consistent with earlier results of error analysis.

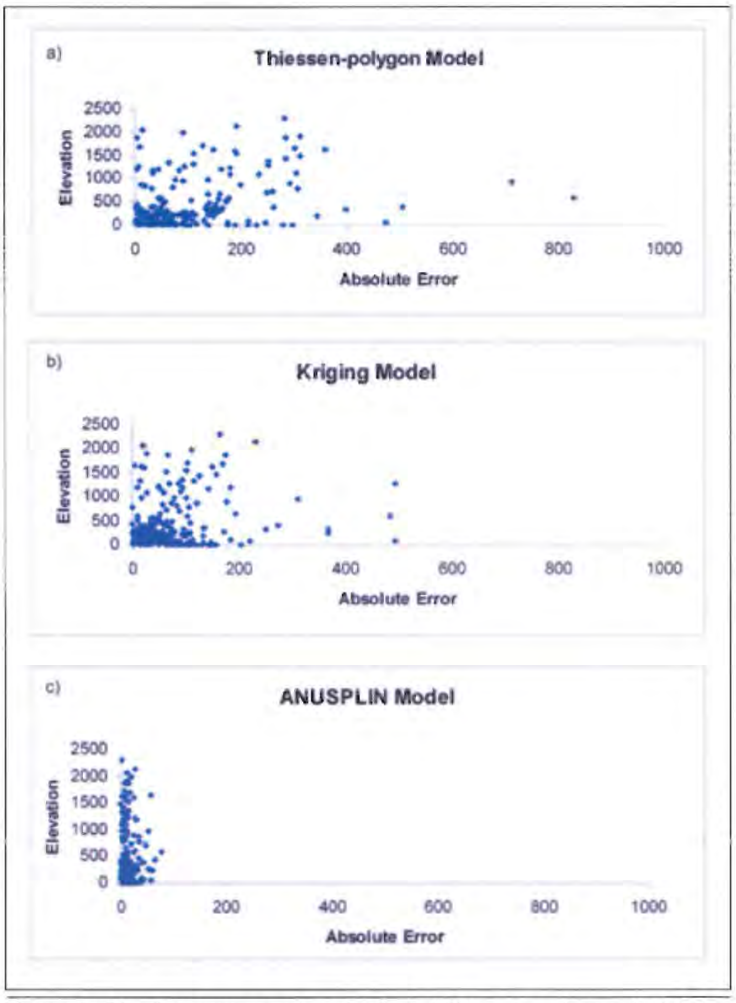

Figure 5. Absolute error vs. elevation for (a) Thiessen polygon, (b) kriging, and (c) ANUSPLIN models.

County Model of Potential UV Exposure

Figure 8 displays a model of potential UV exposure by county for the continental U.S. that was generated through an aggregation of the ANUSPLIN model predictions. Although the geographic patterns of potential UV exposure mimic those generated at 1 km² resolution, it is possible that some variation was lost through aggregation to the county level. The percentage of variation in UV exposure that existed in each county prior to aggregation is illustrated in Figure 9. The maximum coefficient of variation equals 17 percent, and its distribution across counties is non-uniform. These results indicate that the estimates of potential UV exposure for residences located in different areas of the county may be underestimated or overestimated by as much as 17 percent.

The results reported in Table 3 help to identify the potential bias in exposure estimates that may have been introduced if some counties have predominantly north or south-facing slopes (aspects). These results suggest that north- and south-facing slopes offset each other in 77 percent of the 3,111 counties in the continental U.S., which suggests that negligible bias was introduced from this source. However, in the remaining 23 percent of the counties with predominantly

Cos. Aspect	Counties (%)	Counties (count)	Slope Aspect
>0.5	2.8%	86	Predominantly north facing slopes
0.2 to 0.5	18.5%	577	Moderately north facing slopes
-0.2 to 0.2	77.1%	2400	Equal number of south and north facing slopes
-0.2 to -0.5	1.3%	41	Moderately south facing slopes
< -0.5	0.2%	7	Predominately south facing slopes

Table 3. Percentage of counties with north- or south-facing slopes.

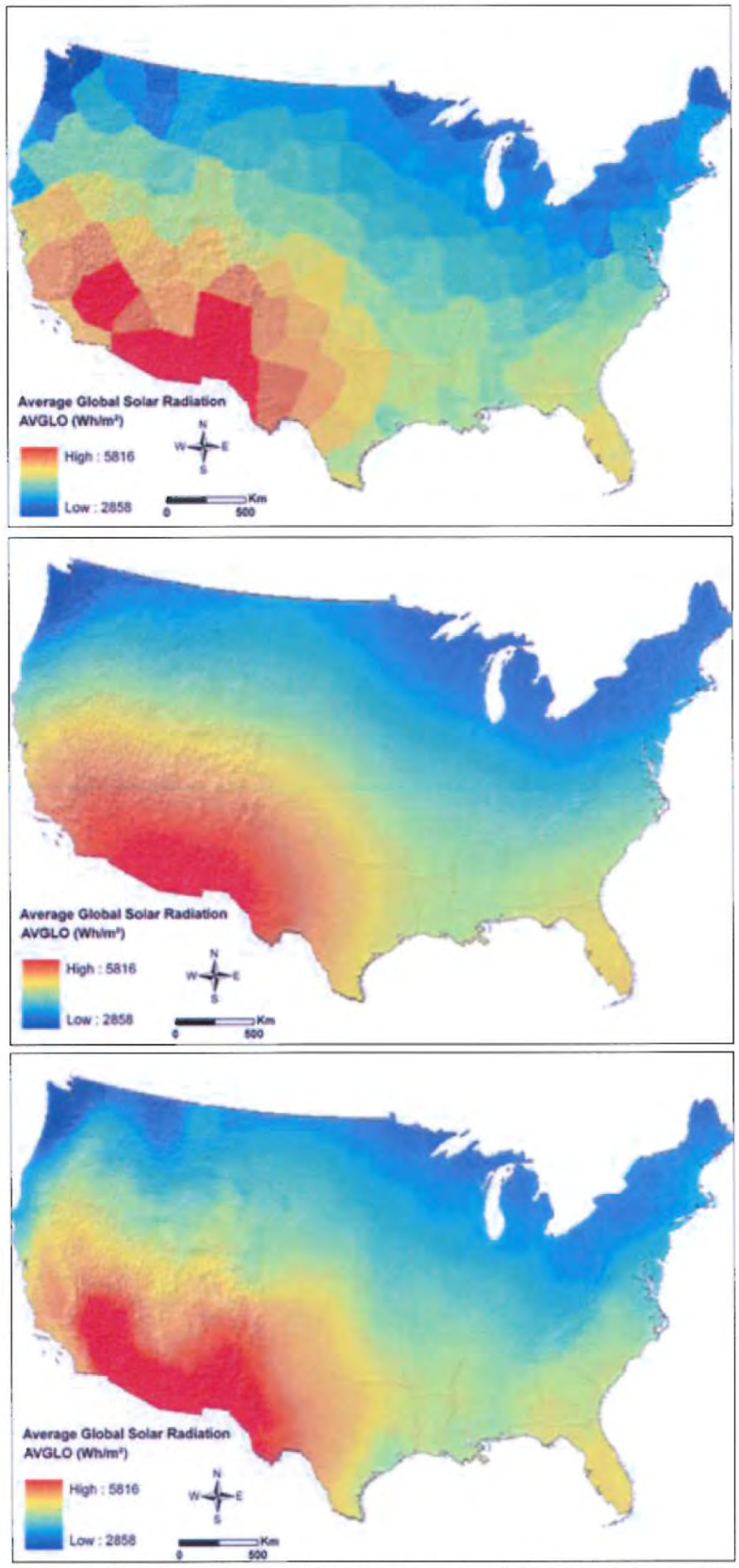

Figure 6. Models of potential UV exposure generated [from top to bottom] by Thiessen polygon, kriging, and ANUSPLIN.

north- or south-facing slopes, the estimates of UV exposure are likely to have been either overestimated or underestimated.

Given that generalization of the UV exposure estimates propagates uncertainty, as indicated by the earlier reported results, it is useful to examine the impact of using inferior model predictions, in this instance Thiessen polygon and kriging, to generate county-level estimates of potential UV. The results of the Wicoxon signed rank test presented in Table 4 indicate that there is a significant difference between the county-level estimates for each pair of models. The differences are more substantial between the Thiessen polygon and kriging than for the other pairs of models.

Discussion

We have compared the performance of the Thiessen polygon and kriging interpolation procedures from the ArcGIS 9 package using an analysis of errors, and the results of this research were compared with the ANUSPLIN spline routine that runs outside the typical GIS toolbox. The most accurate procedure was then used to predict estimates of potential UV exposure at local (1 km^2) and county levels.

The results of the analysis of the accuracy of different interpolation procedures indicate that the Thiessen polygon method generated the highest errors in predicting values at unsampled locations on a non-uniform (elevation-dependent) surface such as radiation. The major difficulty with the Thiessen polygon method is in the assumption that global radiation at all locations within each polygon "belongs" to a particular radiation station within that polygon and, therefore, has the same value. The UVB values change only at the boundaries, and since there is only one observation per polygon, no

within-area variation can be estimated (see Gold 1991 for details). Consequently, the Thiessen polygon interpolation cannot account for the spatial dependence of solar radiation values on elevation, which is a likely reason for the comparatively higher errors in exposure estimates generated by this method.

Universal kriging performed slightly better than the Thiessen polygon method, while ANUSPLIN proved better than both GIS-based routines. The ANUSPLIN model produced results with the smallest mean absolute error, smallest variance of error, smallest root mean square error, the highest correlation coefficient between predicted and observed values, and the smallest correlation between errors and observed values. All of these measures indicate that less uncertainty was associated with predictions done by the ANUSPLIN model.

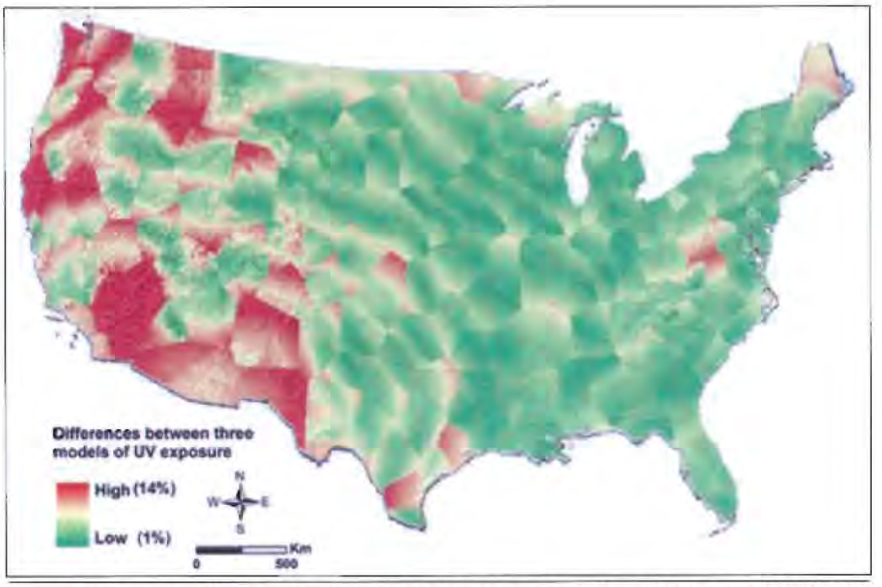

Figure 7. Largest differences between the Thiessen polygon, kriging, and ANUSPLIN exposure surfaces.

Wlcoxon Test Statistics	Kriging/ANUSPLIN	Thiessen/ANUSPLIN	Thiessen/Kriging
Z	-5.798	-5.039	-10.992
Asymp. Sig. (2-tailed)	0.000	0.000	0.000

Table 4. Wilcoxon test for the differences between county estimates of UV exposure.

Several of the advantages of using ANUSPLIN for precipitation modeling also apply to radiation modeling; hence ANUSPLIN also appears to be more suitable for modeling solar radiation than do the Thiessen polygon and kriging methods. The ANUSPLIN method does not depend on prior, climatologically extracted covariances and does not assume that the spatial covariance is stationary. Kriging methods do, and they are hampered by *ad hoc* assumptions about the form the variogram should take as well as computational difficulties in assessing the merit of different functional forms (Hutchinson 1991b, p. 106). Furthermore, ANUSPLIN does not depend on subjective decisions about weighting functions because the program automatically minimizes generalized cross-validation (GVC). Finally, no radius of influence of an input solar radiation (precipitation) station is required, and the spatial distribution of the points may be irregular. Kriging has all these requirements (see Custer et al. 1996 for additional discussion of these issues). The principal value of the exposure map generated based on ANUSPLIN predictions (Figure 6c) lies in its ability to uncover subtle changes in solar radiation exposure.

It should be noted, however, that the accuracy of exposure estimates generated by ANUSPLIN at the scale of 1 km^2 may not remain the same once these estimates are aggregated to a different scale, such as the county level, as we have done in this research. The aggregation may have introduced additional errors in exposure estimates at the county level. As Figure 8 shows, the changes in UV exposure are not as subtle as those at the 1 km^2 grid cell resolution (Figure 6c), and abrupt changes in UV exposure occur at the boundaries between relatively large counties, which is probably not the case in reality. The measurement of the percentage of variation lost once estimates are aggregated to the county level, however, provides an indication of the extent to which the results of subsequent epidemiological analysis of UV exposure may be biased.

Another source of uncertainty in the county-level estimates is that as many as 23 percent of counties have predominantly north- or south-facing slopes, which indicates the possibility that the estimates of UV exposure in those counties are either under-

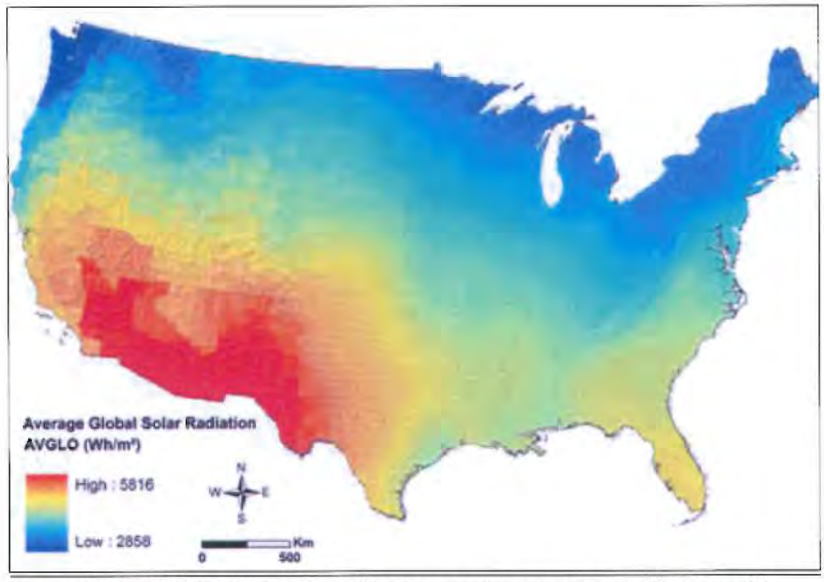

Figure 8. An ANUSPLIN model of UV exposure by county in continental USA.

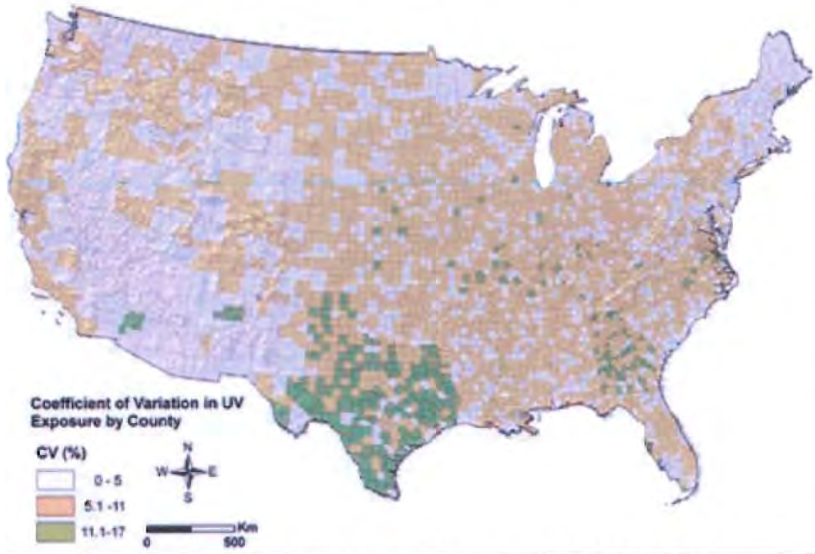

Figure 9. Variation in UV exposure estimates generated by ANUSPLIN.

estimated (north facing) or overestimated (south facing). Terrain modeling techniques are available which take aspect into account (e.g., Wilson and Gallant 2000), but they were not utilized for this research because the county was used as a unit of residential location, and there was consequently no way to relate site-specific effects to specific residential locations.

Conclusions

The results presented in this paper suggest that different interpolation methods can produce different patterns of UV exposure and significantly different estimates. This implies that the use of alternative methods to measure potential UV exposure may have differential impacts on the conclusions about the effects of UV exposure on melanoma and other health effects related to UV exposure. The assessment of performance accuracy of different interpolation methods should, therefore, be conducted before attempting to objectively assess the effects of potential UV exposure at places of residence on health outcomes.

The ANUSPLIN procedure proved to be a relatively simple and computationally efficient method for coping effectively with the potentially large degree of local variation at the resolution of 1 km²; it delivers results that are reproducible and for which the uncertainty is known. Our further research will use county-level estimates of UV exposure computed from ANUSPLIN model predictions in order to build a GIS- based historical UV exposure model and examine, in a case-control setting, the relative importance of UV exposure, compared to self-reported time spent outdoors in melanoma etiology.

ACKNOWLEDGMENTS

Travel funds provided by the University Consortium of Geographic Information Science (UCGIS) and USC GIS Research Laboratory to present an earlier version of this paper at the 2005 UCGIS Summer Assembly are gratefully acknowledged. The current draft benefited greatly from the comments and suggestions of two anonymous reviewers. Dr Cockburn was supported in part by Federal funds from the National Cancer Institute, National Institutes of Health, Department of Health and Human Services, under Contract No. N01-PC-35139, and by Grant No.U55/CCU921930-02 from the Centers for Disease Control and

Prevention. This work was supported in part by NIEHS grant 5P30 ES07048.

REFERENCES

Armstrong, B. K. 1988. Epidemiology of malignant melanoma: Intermittent or total accumulated exposure to the sun? *Journal of Dermatologic Surgery and Oncology* 14: 835-49.

Armstrong, B. K., and A. Kricker. 1993. How much melanoma is caused by sun exposure? *Melanoma Research* 3: 395-401.

Autier, P., and J.F. Dore. 1998. Influence of sun exposure during childhood and during adulthood on melanoma risk. *International Journal of Cancer* 77: 533-7.

Burrough, P. A. 1986. *Principless of Geographical Information Systems for Land Resources Assessment.* Oxford, U.K.: Clarendon Press.

Burrough, P. A., and R. McDonnell. 2000 *Principles of Geographical Information Systems*. New York, New York; Oxford, U.K.: Oxford University Press.

Caldwell, M. M., and S.D. Flint. 1994. Stratospheric ozone reduction, solar UV-B radiation and terrestrial ecosystems. *Climatic Change* 28: 375-94.

Chiles, J. P., and P. Delfiner. 1999. *Geostatistics: Modeling Spatial Uncertainty*. New York, New York: John Wiley and Sons.

Cressie, N. 2003. *Statistics for Spatial Data*, revised edition. New York, New York: John Wiley and Sons.

Cockburn, M., A. Hamilton, and T. Mack. 2001. Recall bias in self-reported melanoma risk factors. *American Journal of Epidemiology* 153: 1021-6.

Copland, L. 1998. The use of terrain analysis in the evaluation of snow cover over an alpine glacier. In: S. N. Lane, K.S. Richards, and J.H. Chandler (eds), *Landform Monitoring, Modeling and Analysis*. New York, New York: John Wiley and Sons. pp. 385-404.

Corbett, J. D., and S. E. Carter. 1996. Using GIS to enhance agricultural planning: The example of inter-seasonal rainfall variability in Zimbabwe. *Transactions in GIS* 1: 207-18.

Craven, P., and G. Wahba. 1979. Smoothing noisy data with spline functions: Estimating the correct degree of smoothing by the method of generalized cross validation. *Numerical Mathematics* 3: 377-403.

Custer, S. G., P. Farnes, J.P. Wilson, and R. D. Snyder. 1996. A comparison of hand- and spline-drawn precipitation maps for mountainous Montana. *Water Resources Bulletin* 32: 393-405.

De Fabo, E. C., F. P. Noonan, T. Fears, and G. Merlino. 2004. Ultraviolet B but not ultraviolet, a radiation initiates melanoma. *Journal of Cancer Research* 64: 6372-6.

De Gruijl, F. R. 1997. Health effects from solar UV radiation. *Radiation Protection Dosimetry* 72: 177-96.

Diffey, B. L. 1989. *Radiation Measurement in Photobiology*. New York, New York: Academic Press. pp. 136-9.

Dubayah, R. and P. M. Rich. 1995. Topographic solar radiation models for GIS. *International Journal of Geographic Information Systems* 9: 405-19.

Elwood, J. M. 1989. Epidemiology of melanoma: Its relationship to ultraviolet radiation and ozone depletion. In: R. R. Jones and T. Wigley (eds), *Ozone Depletion: Health and Environmental Consequences*. London, U.K.: John Wiley & Sons.

Elwood, J. M., and J. Jopson. 1997. Melanoma and sun exposure: An overview of published studies. *International Journal of Cancer* 73: 198-203.

Elwood, J. M., and H.K. Koh. 1994. Etiology, epidemiology, risk factors, and public health issues of melanoma. *Current Opinion in Oncology* 6: 179-87.

Fears, T. R., C. C. Bird, D. Guerry, R. W. Sagebiel, M.H. Gail, D. E. Elder, A. Halpern, E. A. Holly, P. Hartge, and M.A. Tucker. 2002. Average UVB flux and time outdoors predict melanoma risk. *Cancer Research* 62: 3992-96.

Fu, P., and P.M. Rich. 2000. *The Solar Analyst 1.0 user manual*. Helios Environmental Modeling Institute [http://www.hemisoft.com].

Gold, C. M. 1991. Problems with handling spatial data: The Voronoi approach. *Canadian Institute of Surveying and Mapping Journal* 45: 65-80.

Heywood, I., S. Cornelius, and S. Carver. 1998. *An Introduction to Geographical Information Systems*. Upper Saddle Creek, New Jersey: Prentice Hall.

Holman, C. D., and B.K. Armstrong. 1984. Cutaneous malignant melanoma and indicators of total accumulated exposure to the sun: An analysis separating histogenetic types. *Journal of the National Cancer Institute* 73: 75-82.

Hutchinson, M. F. 1991a. *ANUDEM and ANUSPLIN User Guides*. Centre for Resource and Environmental Studies Miscellaneous Report 91/1. Australian National University, Canberra, Australia.

Hutchinson, M. F. 1991b. The application of thin plate smoothing splines to continent-wide data assimilation. In: J.D. Jasper (ed.), *Data Assimilation Systems*. Australian Bureau of Meteorological Research Report 27, Melbourne, Australia.

Hutchinson, M. F. 1993. On thin plate splines and kriging. *Computing and Science in Statistics* 25: 203-10.

Hutchinson, M. F. 1995. Interpolation of mean rainfall using thin plate smoothing splines. *International Journal of Geographic Information Systems* 9: 385-403.

Hutchinson, M. F. 1998. Interpolation of rainfall data with thin-plate smoothing splines I: Two dimensional smoothing data with short range correlation. *Journal of Geographical Information and Decision Analysis* 2: 152-67.

Hutchinson, M. F., and P.T. Gessler. 1994. Splines—more then just a smooth interpolator. *Geodema* 62: 45-67.

Hutchinson, M. F. 2003. *ANUSPLIN Version 4.3*. Australian National University, Centre for Resource and Environmental Studies, Canberra, Australia.

Johnston, K., J.M. Ver Hoef, K. Krivoruchko, and N. Lucus. 2001. *Using ArcGIS Geostatistical Analyst*. Environmental Systems Research Institute, Inc., Redlands, California.

Krivoruchko, K., and C. A. Gotway. 2004. Creating exposure maps using kriging. [http://www.esri.com/software/arcgis/arcgisextensions/geostatistical/].

Lam, N. 1983. Spatial interpolation methods: A review. *American Cartographer* 10: 129-49.

Laslett, G. M. 1994. Kriging and splines: An empirical comparison of their predictive performance in some applications. *Journal of the American Statistical Association* 89: 391-409.

Linacre, E. 1992. *Climate Data and Resources: A Reference and a Guide*. London, U.K.: Ruthledge. pp. 147-201.

Liou, K. N. 2002. *Introduction to Atmospheric Radiation*. New York, New York: Academic Press.

Meyers, D. E. 1994. Spatial interpolation: An overview. *Geoderma* 62: 17-28.

Siska, P. P., and I.K. Hung. 2001. Assessment of kriging accuracy in the GIS environment [http://gis.esri.com/library/userconf/proc01/professional/papers/pap280/].

Stillman, S. T. 1996. A comparison of three automated precipitation simulation models: ANUSPLIN, MTCLIM-3D, and PRISM. M.S. Thesis. Department of Earth Sciences, Montana State University, Bozeman, Montana.

Tevini, M. 1993. *UV-B Radiation and Ozone Depletion, Effects on Humans, Animals, Plants, Microorganisms and Materials*. Boca Raton, Florida: Lewis Publications.

Wahba, G. 1980. Spline bases, regularization and generalized cross validation for solving approximation problems with large quantities of noisy data. In: W. Cheney (ed.), *Approximation Theory III*. New York, New York: Academic Press. pp. 905-12.

Wilson, J. P., and J.C. Gallant. 2000. Secondary topographic attributes. In: J.P. Wilson and C. Gallant (eds), *Terrain Analysis*. New York, New York: John Wiley and Sons. pp. 87-113.